



Article

Calcium Carbonate Mineralization of Microalgae

Panagiota D. Natsi^{1,2} and Petros G. Koutsoukos^{1,2,*} ¹ Institute of Chemical Engineering Sciences, FORTH/ICE-HT, 26500 Patras, Greece² Laboratory of Inorganic & Analytical Chemistry, Department of Chemical Engineering, University of Patras, 26500 Patras, Greece

* Correspondence: pgk@chemeng.upatras.gr

Abstract: Biological substrates catalyze the nucleation and growth of sparingly soluble salts however, the underlying mechanism is largely unknown. In the present study, the growth of calcium carbonate (CaCO₃), on *Acutodesmus obliquus* (AO) microalgae was investigated. The test microalgae favored the growth of CaCO₃ from solutions supersaturated with respect to calcite ($7.94 < SR_{\text{calcite}} < 104.71$). The precipitation of calcite on AO was not preceded by measurable induction times, and the rates of calcite crystal growth were higher for higher microalgae cell concentrations. The presence of the microalgae cultivation medium and illumination of the supersaturated solutions accelerated the precipitation of CaCO₃, increasing the rate by 75% in comparison with the respective value in its absence. AO cultures, air dried at 25 °C yielded higher precipitation rates, in comparison with the respective rates in the presence of active AO cultures. At 70 °C, nucleation and growth were suppressed, due to the destruction of the molecular structure of the microalgae. The CaCO₃ precipitation rates on calcite precipitated on air-dried AO culture, were doubled in comparison with the respective rates obtained with the respective quantities of each component of the composite substrate.

Keywords: calcium carbonate; mineralization; microalgae; precipitation; rate of

**Citation:** Natsi, P.D.;

Koutsoukos, P.G. Calcium Carbonate Mineralization of Microalgae.

Biomimetics **2022**, *7*, 140. <https://doi.org/10.3390/biomimetics7040140>

Academic Editors: Hermann Ehrlich and Teofil Jesionowski

Received: 30 August 2022

Accepted: 21 September 2022

Published: 23 September 2022

Publisher's Note: MDPI stays neutral with regard to jurisdictional claims in published maps and institutional affiliations.



Copyright: © 2022 by the authors. Licensee MDPI, Basel, Switzerland. This article is an open access article distributed under the terms and conditions of the Creative Commons Attribution (CC BY) license (<https://creativecommons.org/licenses/by/4.0/>).

1. Introduction

Membrane fouling in water and wastewater treatment, industrial equipment, and marine equipment [1,2] is a common and persistent problem. Bacteria and microorganisms may form thin biofilm layers on the surfaces they are in contact. Biofilms consist of aggregates of microbial cells adhering on surfaces, encapsulated in polysaccharide matrices. The nature and extent of deposit formation varies according to the local environment, which determines their structural characteristics [3].

The formation of deposits of biological origin (biofouling) is often associated with deposits of insoluble inorganic salts. The relationship between the organic matrix and the inorganic precipitates presents a challenge in modern research. Biofouling, refers to the accumulation of undesired biological material, originating from micro and macro-organisms, on surfaces in the form of biofilms. Composite deposits, consisting of bio-deposits associated with crystalline mineral salts form even though there is no crystallographic affinity [4].

The main biofouling mechanism starts with the fluid flow-driven transport of microorganisms. Next, the microorganisms attach with electrostatic interactions to surfaces, forming biofilms [5–7]. The formation of biofilms is followed by the growth of microorganism cells on the surface, through the consumption of nutrients present in the solution. The extracellular polymeric substances (EPS) are instrumental in the formation of biofilm. They are mainly secretions of microorganisms with high molecular weight, composed of polysaccharides, proteins, nucleic acids, and lipids [8]. EPS provides for the interconnection of microorganisms, resulting in the formation of a three-dimensional matrix. As a result, EPS plays an important role in the physicochemical characteristics of the microorganism aggregates: mass transfer, surface characteristics, and their ability to be attached to surfaces [9,10].

Contact of aquatic systems with atmospheric carbon dioxide and the presence of photosynthetic microorganisms, in combination with relatively high levels of calcium concentrations often results in the formation of calcium carbonate (CaCO_3) deposits associated with photosynthetic microorganisms. The formation of calcite, the thermodynamically most stable polymorph of CaCO_3 , in supersaturated solutions, caused by the presence of microbial cells, biosynthetic products, or products of their metabolic activity, is known as microbially induced calcite precipitation (MCIP) [11]. Bicarbonate (HCO_3^-) and calcium ions, produced through metabolic activity do contribute to the formation of calcite in the microenvironment of the microbial cells [12]. Despite the fact, that the formation of calcite, has been reported only in association with extracellular components, several studies suggested that intracellular CaCO_3 precipitation takes place in cyanobacteria as well [13]. Head et al. (2000) reported that calcite may precipitate intracellularly [14]. More recently, Xu et al. (2019) reported calcite and aragonite precipitation, via cell membrane lysis, induced in cyanobacteria [15].

Cell surfaces are very efficient for carbonate nucleation and crystal growth. Cell walls with negatively charged functional groups, such as carboxyl, phosphate, and amino groups, are capable of adsorbing metal ions [10]. For example, the cell wall of *Bacillus subtilis* can bind a significant amount of Mg^{2+} , Fe^{3+} , Cu^{2+} , Na^+ , K^+ , Mn^{2+} , Zn^{2+} , Ca^{2+} , Au^{3+} , and Ni^{2+} ions [16]. Moreover, metabolic processes during the growth of microorganisms, play a crucial role in the formation of CaCO_3 [17]. Depending on the environment, in which MCIP takes place, a corresponding metabolic process is likely to be the determining factor. The presence of *Acutodesmus obliquus* (AO) in freshwater resulted in the production of rather high lipids concentrations increasing respectively the concentration of carboxyl groups [18]. Relatively little however is known concerning the mechanism of the mineral phase formation in the presence of photosynthetic microalgae like AO. The presence of AO in solutions supersaturated with respect to calcium carbonate may provide additional active sites for nucleation and growth. In the present study we investigated the mechanism of the formation of CaCO_3 in the presence of AO from measurements of the kinetics of precipitation of calcite in the presence of AO in supersaturated solutions. The most important factors involved with the heterogeneous nucleation and crystal growth of calcite in the presence of these biological substrates were calculated from the kinetics data. The stability domain of the CaCO_3 supersaturated solutions was investigated at free drift conditions. More precise measurements of the rates of precipitation were done at constant supersaturation, in which the thermodynamic driving force for the precipitation of CaCO_3 was kept constant.

2. Materials and Methods

2.1. *Acutodesmus obliquus* (AO) Culture Development

The freshwater microalgae AO was selected for the experiments, as a typical representative of photosynthetic microalgae. These microalgae strains were identified in the water bodies contaminated with industrial effluents [19]. The AO culture was obtained from the Culture Collection of Algae at Göttingen University (*Sammlung von Algenkulturen der Universität Göttingen*, SAG) (Strain number 276-1). Cultures of this green photosynthetic microalgae were grown in a specific culture medium. Following the preparation of the Basal Bolds culture Medium (BBM) [20], the microalgae population was grown in 250 mL conical flasks (batch cultures) (Figure 1a). The composition of the culture medium is shown in Table 1. The supersaturated solutions, upon inoculation with AO cultures, were enriched with nutrient components, the final concentration of which is also shown in Table 1. Air was continuously pumped through the batch cultures, while the illumination conditions selected favored the growth of microorganisms. Cold white 3500 lx lamps were used. Cultures were grown at 25 ± 2 °C and the pH was adjusted to 6.5 with standard solution 0.1 M NaOH.

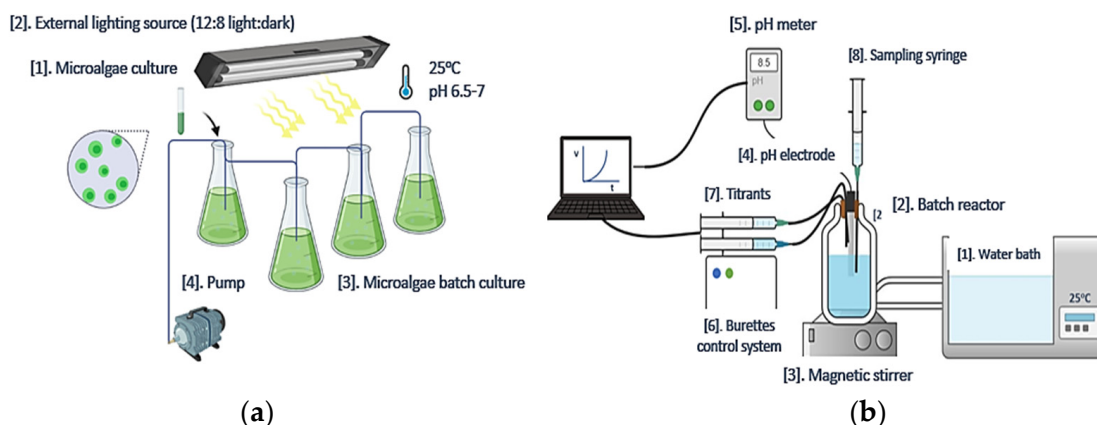


Figure 1. Experimental setup for (a) AO culture preparation and (b) Experimental setup for the mineralization experiments.

Table 1. Composition of modified AO culture medium suitable * for the supersaturated CaCO_3 solutions.

Component	Concentration/mM
$\text{MgSO}_4 \cdot 7\text{H}_2\text{O}$	0.400
KNO_3	0.247
NaNO_2	0.005
H_3BO_3	0.040
$\text{FeCl}_3 \cdot 2\text{H}_2\text{O}$	0.006
$\text{MgSO}_4 \cdot 7\text{H}_2\text{O}$	0.400

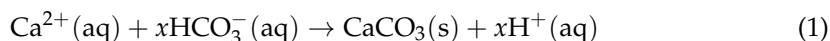
* Modification from the recommended optimal concentrations for the AO culture so that the supersaturated solutions were stable and did not result in the precipitation of magnesium or iron carbonates.

Four cultures were grown for comparison reasons and measurement of chlorophyll concentration spectrophotometrically.

2.2. Precipitation of CaCO_3 in Supersaturated Solutions

Calcium carbonate (CaCO_3) precipitation was studied in solutions, supersaturated with respect to all CaCO_3 anhydrous polymorphs. The experimental setup is shown in Figure 1b. The supersaturated solutions were prepared in a double-walled glass (Pyrex[®]) reactor, thermostated at 25.0 ± 0.2 °C. by the circulation of water of a thermostat through the walls of the reactor. Sodium bicarbonate (NaHCO_3) and sodium carbonate (Na_2CO_3) stock solutions were prepared from the respective crystalline solids (Merck, Puriss.) by dissolution in triply distilled water. The solutions were filtered through 0.2 μm membrane filters (Millipore, Bedford, MA, USA) and were used without further standardization. Fresh solutions were prepared for each experiment. Calcium chloride stock solutions were prepared from calcium chloride dihydrate salt (Merck, Kenilworth, NJ, USA, Puriss.). The stock solutions were standardized with titration with 0.1 M Ethylenediaminetetraacetic acid (EDTA), standard solution, pH 10 with $\text{NH}_3/\text{NH}_4^+$ buffer solution, with murexide indicator, and by atomic absorption spectrometry (AAS, AAnalyst 300, Perkin Elmer, Norwalk, CT, USA). The supersaturated solutions were prepared by mixing equal volumes of calcium chloride and sodium bicarbonate stock solutions. The solution's pH was adjusted to 8.5 with 0.1 M NaOH standard solution, standardized with potassium hydrogen phthalate. Next, the supersaturated solutions were inoculated with known volumes of suspensions of AO cultures so that the number of AO cells introduced in the reactor was known. Alternatively, the supersaturated solutions were inoculated with weighted amounts of solids. Dry AO culture (dried at 25 or 70 °C), CaCO_3 crystals on which microalgae was grown, and CaCO_3 which was precipitated on air dried AO culture. Calcite was used as the reference system since in this case there is no nucleation energy barrier and crystal growth

started immediately on the calcite crystals upon their suspension in the supersaturated solutions. For this reason, calcite crystals were prepared by precipitation and aging (the specific surface area was $0.33 \text{ m}^{-2} \cdot \text{g}^{-1}$). Calcite precipitation was accompanied by a decrease in the pH value of the supersaturated solutions, because of the release of protons:



Two different methods were used. The first, known as the free-drift method, mainly aimed to measure the metastable zone width (MZW) for the CaCO_3 solutions depending on the inoculating material. In this method, the induction time for the onset of precipitation was measured from the time elapsed between the preparation of the supersaturated solutions till the beginning of the solution's pH drop. The second methodology aimed at accurately measuring the rates of precipitation since accurate measurements are needed for the investigation of the mechanism.

2.2.1. Precipitation of CaCO_3 from Supersaturated Solutions: Free-Drift Method

Once precipitation in the supersaturated solutions started, the activities of all ions in the supersaturated solutions decreased (Equation (1)). The variation of key parameters was monitored. Solution pH was recorded as a function of time. Samples were withdrawn (with the higher frequency following the start of precipitation and lower closer to completion as indicated by the pH changes, monitored in real-time, and recorded), filtered through membrane filters ($0.2 \mu\text{m}$ Millipore) and the filtrates were acidified, and then analyzed for calcium with atomic absorption spectrometry (AAS, Perkin Elmer AAnalyst 300). The decrease of all parameters continued until no further macroscopic change was observed. At the end of the precipitation process, the suspension in the reactor was filtered and the solid on the filters was characterized by powder X-ray diffraction (XRD, Siemens D-500, Frankfurt, Germany) and scanning electron microscopy (SEM, Leo Supra with Bruker XS EDX microanalysis unit, Zeiss, Oberkochen, Germany). Infra-Red spectra (Attenuated Total reflection—Fourier Transformed Infra-Red, ATR-FTIR) of the solid were recorded in Nicolet 6700 spectrometer (Thermo Scientific, Waltham, MA, USA) equipped with a diffuse reflectance (DRIFTS) cell (Spectra Tech, Thermo Scientific, Waltham, MA, USA).

2.2.2. Precipitation of CaCO_3 at Constant Supersaturation

Solution pH dropped by as little as 0.01 units, triggering the addition of titrant solutions from two mechanically coupled burettes, mounted on a motorized syringe pump. The two burettes contained calcium chloride and carbonate solutions at concentrations calculated so that they had the stoichiometry of Calcium:Carbonate = 1:1, as in the precipitating solid. As a result, the activities of all ions in the solutions and hence, the respective supersaturation was kept constant. The volume of the titrants added, as a function of time, needed to keep the supersaturation constant, was recorded and from the corresponding graphs, the deposition rates of CaCO_3 were calculated. sampling was done randomly during precipitation and at the end of the crystal growth, as described in Section 2.2.1.

3. Results

3.1. Measurement of Growth Rate of Microalgae AO

Microalgae cultures were grown in 250 mL conical flasks under appropriate illumination and aeration conditions to achieve an optimum growth rate [20]. Samples were withdrawn from the culture suspensions, at regular intervals, and the optical density of the aqueous phase, separated from the solids by filtration, was measured at 650 nm. The optical density is a measure of the concentration of (total) chlorophyll produced during algal growth. AO growth rate was calculated from the change in total chlorophyll concentration in the aqueous phase of the culture. The change in chlorophyll concentration is shown in the plot in Figure 2.

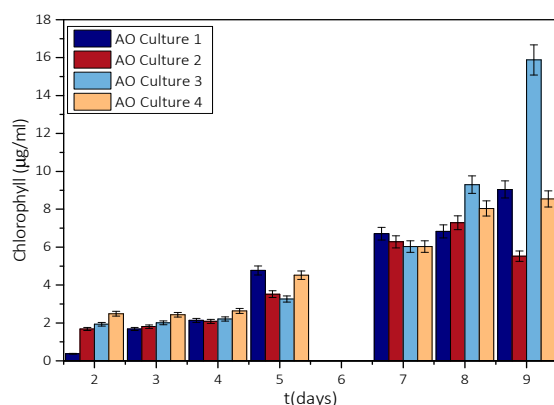


Figure 2. Variation of total chlorophyll with the time of different AO cultures.

As may be seen, chlorophyll in the aqueous phase of the culture increased with time exponentially. From the measurements of chlorophyll concentration, the growth rate of the microalgae was calculated from the slope of the logarithm of the chlorophyll produced as a function of time, equal to $2 \mu\text{g}\cdot\text{h}^{-1}$. The rates measured were lower (about three orders of magnitude) in comparison with the literature report [21], but it was sufficient to provide sufficient biomass for use as a substrate in the nucleation and crystal growth part of the study.

For the calculation of the rate of growth of AO, the cell population was measured by counting the number of microalgae cells, using a hemocytometer. During the measurements, sampling was done directly from the culture. A few μL was placed on the plate of the hemocytometer (Neubauer plate), covered with a glass surface, to immobilize the cells. Using an optical microscope ($\times 40$) and a camera, photographs were taken (Figure 3) for about a week, during which the microalgae cell population was counted using ImageJ[®] software [22]. The morphological characteristics of different cultures, grown in different batches were identical.

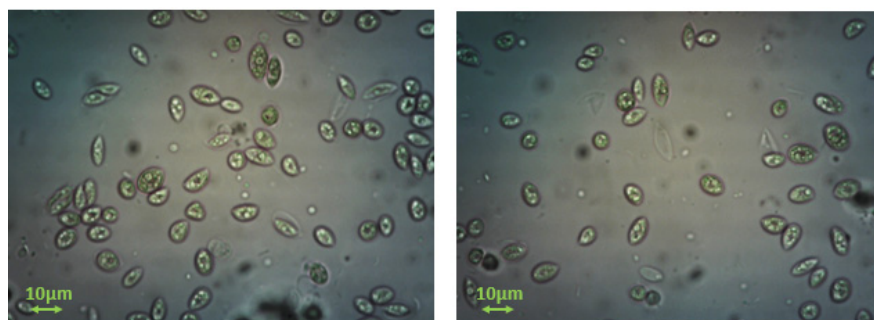


Figure 3. Optical microscope photographs of two different AO cultures ($\times 400$) show the same morphological characteristics.

From the population measurements, the concentration (number of cells per mL) was calculated, and the results are shown in Figure 4. As may be seen, the population increase was exponential during the first three days. Past the 5th day, it showed a stabilization trend, in agreement with the optical density measurements. Moreover, the transition of the microorganism to the stationary phase of its growth was confirmed.

The ATR-FTIR spectra (A) of dried *Acutodesmus obliquus* are shown in Figure 5. The absorbance band between 3500 and 3000 cm^{-1} was typically related to hydroxyl groups. The two intensive bands on 2850 and 2925 cm^{-1} corresponded to CH_2 symmetric and asymmetric open stretch vibrations. The bands from 1030 to 1541 cm^{-1} correspond to a methyl group stretch assigned to O-CH_3 . The band around 1643 cm^{-1} corresponded to asymmetric vibrations assigned to the $-\text{CH}_3$ group [23,24].

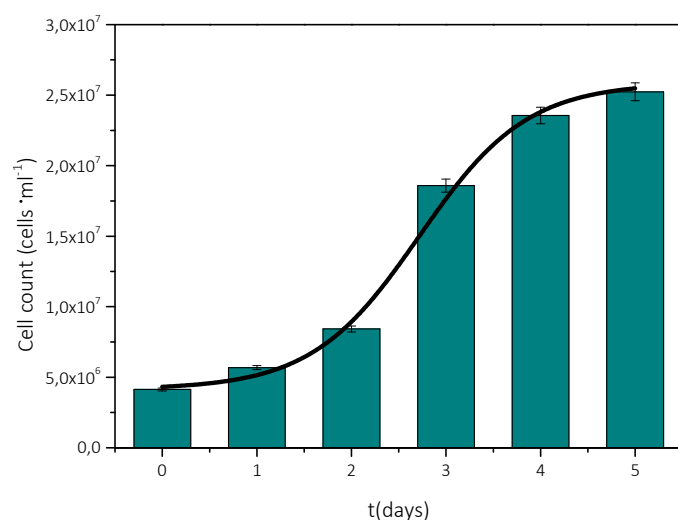


Figure 4. AO culture cell density as a function of time.

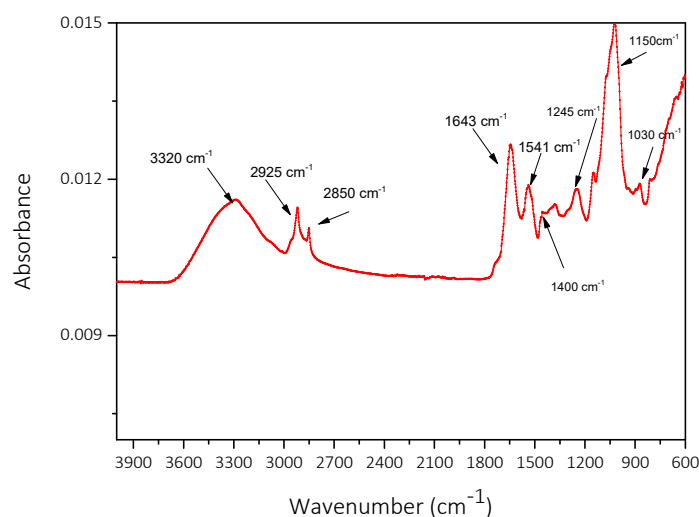


Figure 5. ATR-FTIR spectrum of *Acutodesmus obliquus* dried at 25 °C.

The infrared spectra of the dried AO culture were in good agreement with literature reports of the ATR-FTIR spectra of chlorophyll and *Chlorella vulgaris* microalgae [23]. It has been shown that lipid membranes have a substantial calcium-binding capacity, with several types of binding sites present [25]. The significant presence of lipids in AO cultures is therefore expected to promote nucleation and growth of CaCO_3 as calcium binding may favor the development of active sites for CaCO_3 growth on the lipid membranes.

AO microalgae cultures were grown on calcite, the thermodynamically most stable CaCO_3 polymorph. Specifically, calcite powder was suspended into microalgae culture suspensions during the early stages of their growth. Alternatively, CaCO_3 was precipitated spontaneously by the addition of calcium chloride and sodium carbonate solutions in the culture medium at equimolar, final concentrations of 0.2 M each, pH 8.5. The BET-specific surface area (SSA) of the mechanical mixture of calcite with the AO culture in suspensions, followed by drying at 25 °C was $0.4 \text{ m}^2 \cdot \text{g}^{-1}$. The SSA of the solid prepared by the spontaneous precipitation of calcite on air-dried AO culture was $2.2 \text{ m}^2 \cdot \text{g}^{-1}$. The morphology of calcite crystallites following the growth of the AO culture did not show significant changes. Small size particles (ca. 50 nm), corresponding to the AO culture cells, were evenly distributed on the flat faces of the rhombohedral calcite crystals (Figure 6a,b).

The crystallites of the solid formed during the precipitation of calcite in suspensions of air-dried AO culture suspended in the supersaturated solutions consisted of hollow

vaterite crystallites, confirmed by XRD analysis (Figure 6c,d). The stabilization of the thermodynamically unstable polymorph, vaterite, was possibly due to the presence of soluble organic compounds in the supersaturated solution in which precipitation took place.

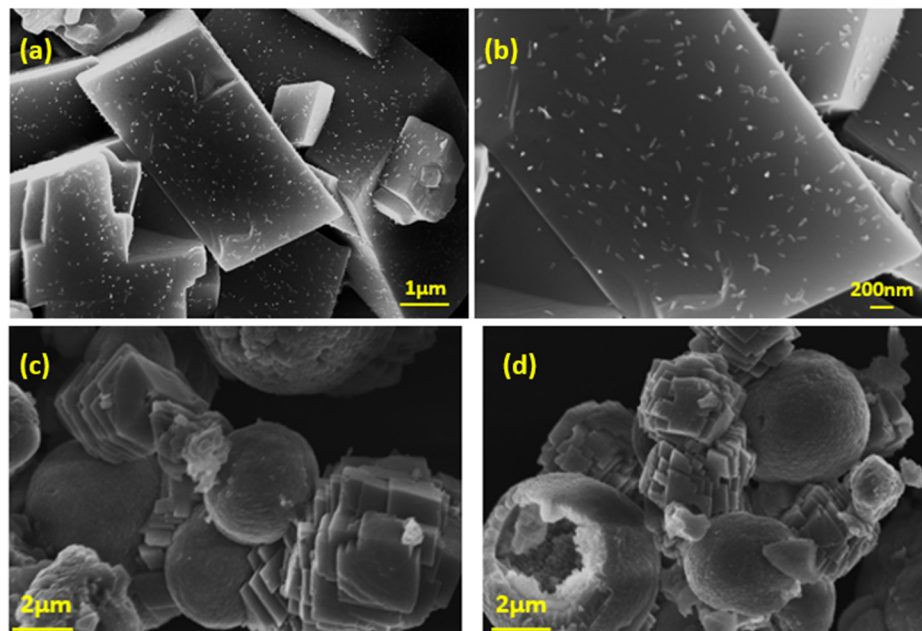


Figure 6. Scanning electron microscope (SEM) photographs (a), (b) of microalgae cells grown and/or attached to flat faces of rhombohedral calcite crystals (c), (d) CaCO_3 spontaneously precipitated on dried AO culture suspended in supersaturated solutions.

Examination of the morphology of the composite calcite- AO with SEM (Figure 7) showed that CaCO_3 , precipitating in the suspension of the air-dried AO culture cells in the supersaturated solution, revealed considerable affinity between the organic-inorganic phases. As may be seen in the SEM pictures shown in Figure 7, calcite crystals with the characteristic rhombohedral morphology (shown better on the left picture), grow on chains of AO aggregates.

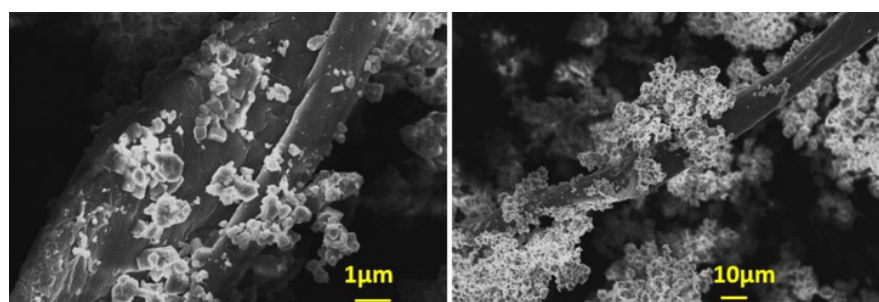


Figure 7. Scanning electron microscope (SEM) photographs of CaCO_3 deposited in suspensions of dry microalgae.

3.2. Spontaneous Precipitation of CaCO_3 in Supersaturated Solutions: The Metastable Zone Width

3.2.1. The Effect of the Presence of AO Culture Cells in the Supersaturated Solutions

Since the ATR-FTIR study of the dried AO cultures revealed the presence of lipids, it is possible that the presence of AO cultures in supersaturated solutions of CaCO_3 may favor the selective overgrowth of CaCO_3 , through interactions that may increase the active growth sites in.

Solution supersaturation is the thermodynamic driving force for the precipitation of CaCO_3 polymorphs from supersaturated solutions. The supersaturation ratio (SR), or

saturation index (SI) is defined as the ratio of the ion activity product for the salt considered over the respective thermodynamic solubility product. For the CaCO₃ polymorphs (vaterite, aragonite, calcite in the order of increasing thermodynamic stability):

$$SR = \frac{(Ca^{2+})(CO_3^{2-})}{K_{S,X}^O} \quad (2)$$

In Equation (2) () denotes activities of the enclosed ions and $K_{S,X}^O$ is the thermodynamic solubility product of polymorph x. The relative supersaturation with respect to polymorph x, σ_x , is defined as

$$\sigma_x = SR^{1/2} - 1 \quad (3)$$

Ion activities in the supersaturated solutions were calculated taking into consideration all equilibria involved, using equilibrium calculations in aqueous systems software, PHREEQC [26].

The supersaturated solutions were prepared in two different ways: (a) mixing equimolar calcium chloride and sodium carbonate solutions, followed by the inoculation with nutrient medium (20 mL) and microalgae culture (5–20 mL), and (b) as in (a) with the difference that the solutions contained sufficient nutrients to ensure the growth of AO cultures.

Precipitation of CaCO₃ in the Presence of Different AO Culture Mass

Solutions, supersaturated with respect to all CaCO₃ polymorphs, with a volume totaling 0.100 dm³ were prepared by mixing equal volumes of calcium chloride, sodium bicarbonate, and sodium chloride solutions directly in the reactor, under constant magnetic stirring to ensure homogeneity of the solutions. 20 mL of nutrient medium was added, and the solution pH was adjusted again to 8.5. Next, a quantity of AO culture suspension in the stationary phase of growth was introduced into the stirred solution. The quantities of AO cultures that inoculated the supersaturated solutions were 5, 10, and 20 mL and corresponding to cell numbers 1.26×10^{-6} , 2.52×10^{-6} , and 5.04×10^{-6} cells, respectively. Following inoculation with AO culture, the solution pH was re-adjusted to pH 8.5 as needed. Samples were withdrawn and filtered through membrane filters then the filtrates were analyzed for calcium. The onset of precipitation was identified from concentration changes from the initial values, and it was free drift. The precipitation of CaCO₃ lasted for 24 h when it reached a steady state, which was considered to be the completion of precipitation. In this case, the calculation of initial rates is tricky, because the data collected correspond to different supersaturations, i.e., at different conditions which are often influenced by the transformation of less stable intermediate polymorphs to the most stable calcite. It was therefore preferred to calculate the integral rates of CaCO₃ precipitation from the calcium-time profiles (Figure 8). The experimental conditions are summarized in Table 2.

The concentration of the nutrient medium in the supersaturated solutions was sufficiently low and did not affect the calculated supersaturation with respect to the CaCO₃ polymorphs. It was also assumed that inside the reactor there was no growth of AO (stationary phase). This assumption was validated from measurements of the concentration of AO cells in the reactor, as may be seen from the data summarized in Table 2. As may be seen from the calcium-time profiles shown in Figure 8, the higher the supersaturation, the higher the change of total calcium (Ca_t) over the same time period, in agreement with the calculated integral rates, R_a :

$$R_a = \frac{[Ca_t]_0 - [Ca_t]_t}{\Delta t} \quad (4)$$

In Equation (4) $[Ca_t]_0$ and $[Ca_t]_t$ are the total calcium concentrations at time $t = 0$, before the onset of precipitation, and at time t respectively. The rates were calculated over the time period of 100 min (Δt), when calcium concentration attained a plateau value, suggesting the completion of the precipitation process. As may be seen, in Figure 8 in all cases, and over the range of the relative supersaturation values investigated, the precipitation of

CaCO_3 took place practically without any induction time, regardless of the presence of AO culture. It is interesting to note that inoculation of the supersaturated solutions with calcite crystal, was preceded by induction time (ca. 30 min, Figure 8a,b) which may be attributed to the incomplete dispersion of the crystals. In these solutions the precipitation of CaCO_3 was spontaneous. The presence of AO culture, however, as may be seen, enhanced the precipitation of CaCO_3 at all supersaturations in the range investigated. Both the rates of precipitation and the total amount of CaCO_3 precipitated were higher in the presence of AO cultures with the respective nutrient components from the culture medium. It is interesting to note that the rate of precipitation and the total amount of CaCO_3 precipitated increased with increasing AO culture concentration in the supersaturated solutions, suggesting a direct dependence of the rate of precipitation on the number of active sites present in the AO culture.

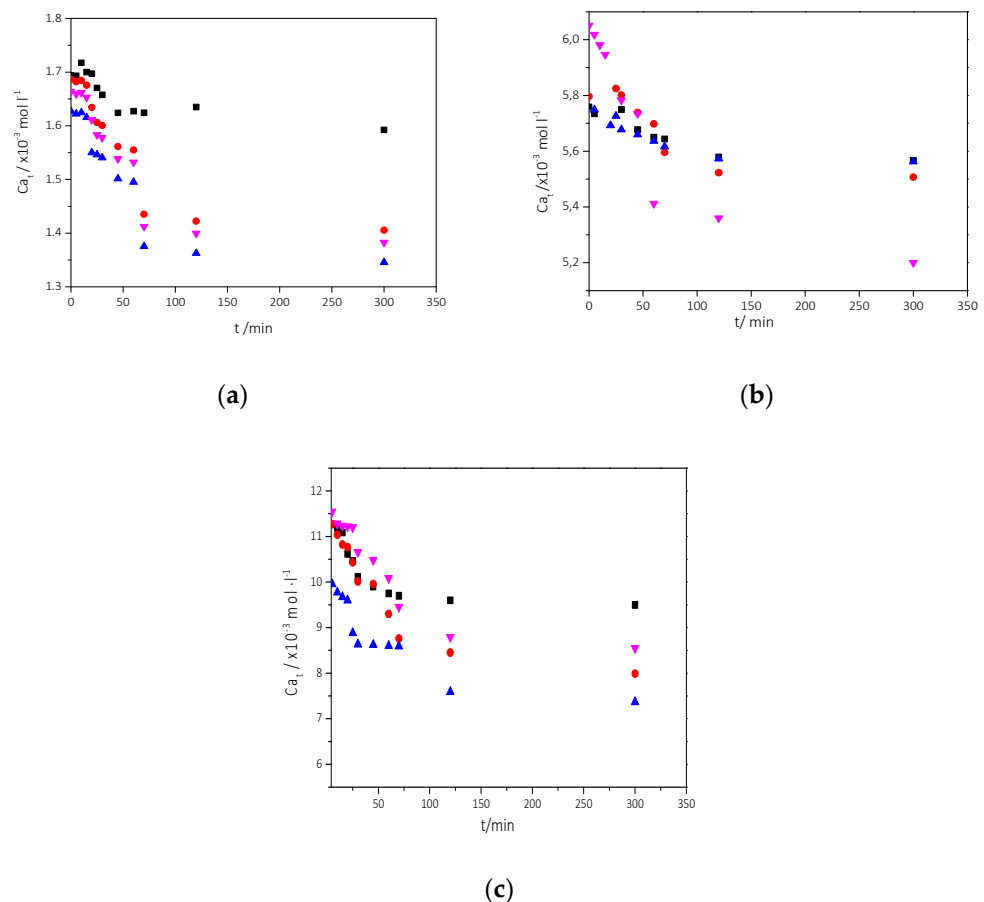


Figure 8. Calcium concentration as a function of time during CaCO_3 precipitation in the presence of 20 mL nutrient medium and microalgae. (a) $\sigma_{\text{calcite}} = 0.68$, (b) $\sigma_{\text{calcite}} = 4.43$, (c) $\sigma_{\text{calcite}} = 9.23$ (■) Absence of microalgae and nutrient (●) presence of nutrient and 5 mL algae (▲) presence of nutrient and 10 mL algae and (▼) presence of nutrient and 20 mL of algae; 25 °C, pH 8.5, NaCl 0.15 M.

As may be seen, the precipitation rate of CaCO_3 was higher when the concentration of microalgae was higher, suggesting that the nucleation and crystal growth of CaCO_3 forming is directly related to the number of AO cells which induce the formation of the mineral. the rate of precipitation increased with increasing supersaturation and the available number of AO cells, as may be seen in Figure 9.

Table 2. Free drift CaCO_3 precipitation in the presence of 20 mL nutrient medium and AO culture. Initial total calcium, Ca_t , concentrations, calculated supersaturation ratio, SR, values with respect to calcite, relative supersaturation with respect to calcite, AO cell concentration and rates of CaCO_3 precipitation (integral rates); 25 °C, pH 8.5, NaCl 0.15 M.

Solution	$\text{Ca}_t/\times 10^{-3}$ $\text{mol}\cdot\text{L}^{-1}$	Supersaturation Ratio, $\text{SR}_{\text{calcite}}$	Relative Supersaturation σ_{calcite}	AO Cell Concentration/ \times $10^7 \text{ cells}\cdot\text{L}^{-1}$	Precipitation Rate, R_p/\times $10^{-7} \text{ mol min}^{-1} \text{ L}^{-1}$
1	1.7	7.94	0.68	1.26	1.4
				2.52	3.5
				5.04	3.6
2	5.8	29.51	4.43	1.26	5.4
				2.52	5.5
				5.04	6.6
3	11.6	104.71	9.23	1.26	26.6
				2.52	34.0
				5.04	37.3

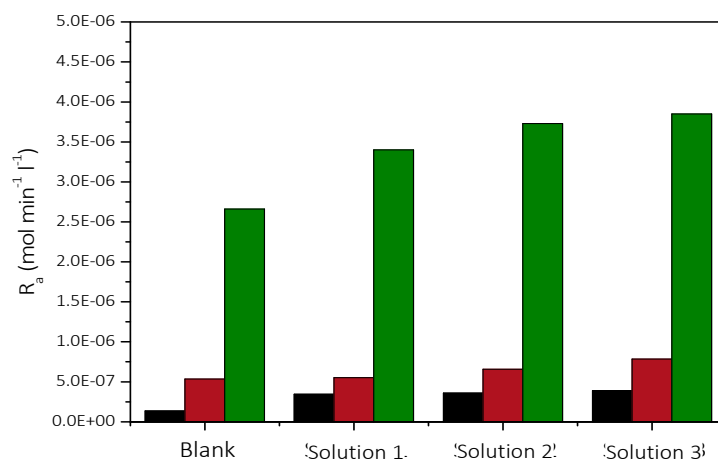


Figure 9. Rates of CaCO_3 precipitation in the presence of 20 mL nutrient medium and microalgae. Solution 1: 5 mL of microalgae, Solution 2: 10 mL of microalgae, Solution 3: 20 mL of microalgae; 25 °C, pH 8.5, NaCl 0.15 M; AO cells concentration: (ν) $1.26 \times 10^{-6} \text{ cells}\cdot\text{L}^{-1}$; (ν) $2.52 \times 10^{-6} \text{ cells}\cdot\text{L}^{-1}$; (ν) $5.04 \times 10^{-6} \text{ cells}\cdot\text{L}^{-1}$.

As may be seen in Figure 10, the dependence of the rate of CaCO_3 precipitation for each of the three supersaturation ratio values studied, on the concentration of AO culture cells in the supersaturated solutions is linear. At the least value of the supersaturations investigated, the rate of precipitation was proportional to the concentration of the AO culture cells in the supersaturated solutions. It is therefore suggested that the AO culture cells provide the active growth sites for the growth of calcite on AO cells and that there is selectivity of calcite growth on the specific type of microalgae cells, mainly consisting of lipids.

The precipitated solid was identified as calcite by XRD (Figure S1, Supplementary Material).

3.2.2. Precipitation of CaCO_3 in the Presence of AO Culture, Illumination, and Nutrient at Constant Supersaturation

Measurements of rates of precipitation and of the related induction times were measured by the constant supersaturation method [27], which allowed for the accurate measurement of both the induction time and of the rates of precipitation. The presence of nutrients in the AO culture medium is necessary for the growth of the respective cells, we have tested the use of modified (lower concentrations of the metal ion components)

nutrient medium (Table 1). This was necessary, to avoid precipitation of metal carbonates other than CaCO_3 (MgCO_3 or FeCO_3 e.g.). In this case, larger volume of the supersaturated solutions and a higher capacity reactor (0.5 dm^3) were used. The supersaturated solutions were prepared in the reactor, as already described, at $25 \pm 0.5 \text{ }^\circ\text{C}$ by mixing equimolar solutions of calcium and carbonate (0.2 dm^3 each), with the simultaneous addition of precisely measured amounts of nutrients (Table 1). The supersaturated solutions with the nutrients were adjusted to pH 8.5 with standard NaOH solution. The solutions were homogenized by magnetic stirring through the precipitation process. 5 mL of the AO culture was injected into the supersaturated solutions. The kinetics of precipitation of CaCO_3 was monitored both in the absence (control) and in the presence of nutrient medium and illumination.

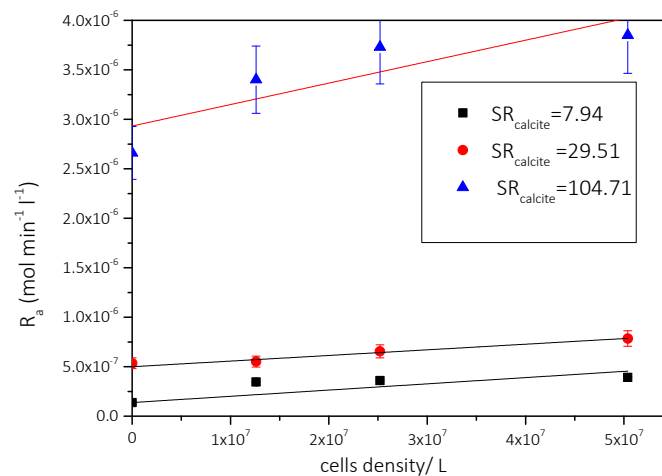


Figure 10. Dependence of the rate of precipitation of CaCO_3 on the cell concentration of AO culture, in the presence of nutrient medium (20 mL/100 mL of supersaturated solution); $25 \text{ }^\circ\text{C}$, pH 8.5, NaCl 0.15 M.

From the volume of titrant solutions added (Figure 11), to maintain constant supersaturation as a function of time, the precipitation rates were calculated according to Equation (4). The measured rates of precipitation of CaCO_3 and the respective solution conditions are summarized in Table 3.

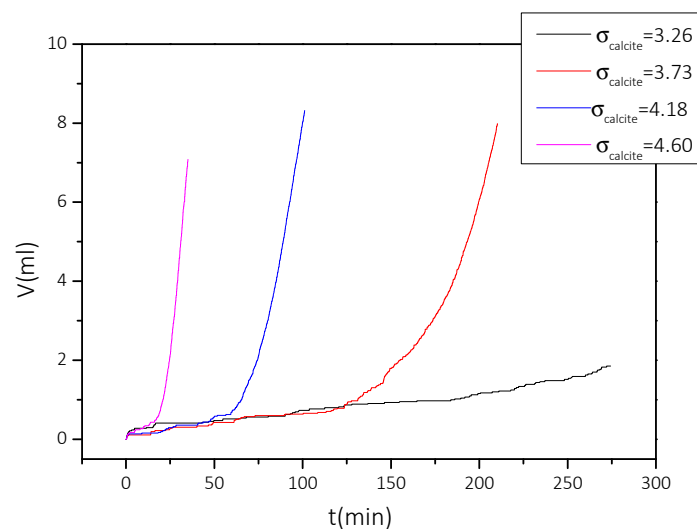


Figure 11. Titrant solution volume added to the reactor to maintain supersaturation, in the presence of medium and 5 mL of algae under illumination, as a function of time: $25 \text{ }^\circ\text{C}$, pH 8.5, NaCl 0.15 M.

Table 3. Precipitation of CaCO_3 in supersaturated solutions at constant supersaturation, in the presence of culture medium and 5 mL of AO culture, under illumination. Calcium (total) concentration in the supersaturated solutions, relative supersaturation with respect to calcite, induction time preceding the onset of precipitation, and the precipitation rate of CaCO_3 ; 25 °C, pH 8.5, NaCl 0.15 M.

$\text{Ca}_t \times 10^{-3} \text{ mol}\cdot\text{L}^{-1}$	Relative Supersaturation, σ_{calcite}	Induction Time, $t_{\text{ind}}/\text{min}$	Precipitation Rate, $R_p / \times 10^{-7}$ $\text{mol}\cdot\text{min}^{-1}\cdot\text{L}^{-1}$
3.5	2.38	150	0.21
4.0	2.84	140	0.24
4.5	3.26	120	1.78
5.0	3.73	116	8.15
5.5	4.18	47	27.5
6.0	4.60	10	79.0

From the data in Table 3, the stability diagram of the supersaturated with respect to calcite solutions was drawn, in the presence of 5 mL of AO culture, nutrient medium, and illumination. The stability diagram is shown in Figure 12. In the same graph, the stability of the supersaturated solutions in the absence of AO culture, is also shown. As may be seen, the presence of the AO culture resulted in a narrower stability zone of the supersaturated CaCO_3 solutions.

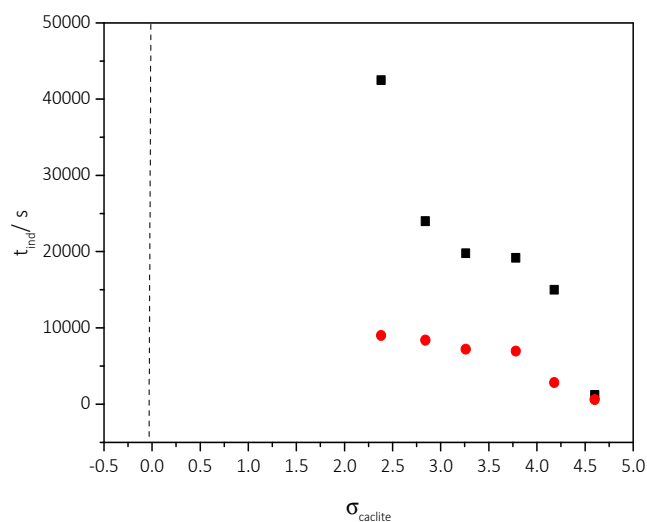


Figure 12. Stability diagrams of CaCO_3 supersaturated solutions, in the presence of medium and 5 mL AO culture slurry, under illumination. Induction time as a function of relative supersaturation. (■) in the absence of AO culture; (●) in the presence of AO culture; 25 °C, pH 8.5, NaCl 0.15 M. Measurements at constant supersaturation.

Up to a relative supersaturation value of about 3.8, there was no significant difference between the rate of CaCO_3 precipitation in the presence or in the absence of AO culture. For relative supersaturation values exceeding 4.3 the rate of CaCO_3 precipitation increased significantly in the presence of AO culture by up to 100% in comparison with the reference value (Figure 13). It may be suggested that the interaction between the free calcium ions with the lipids rich AO cells resulted in the creation of additional active growth sites. Consequently, it may be suggested that locally higher supersaturation was developed on the surface of the AO cells in comparison with the respective in the bulk.

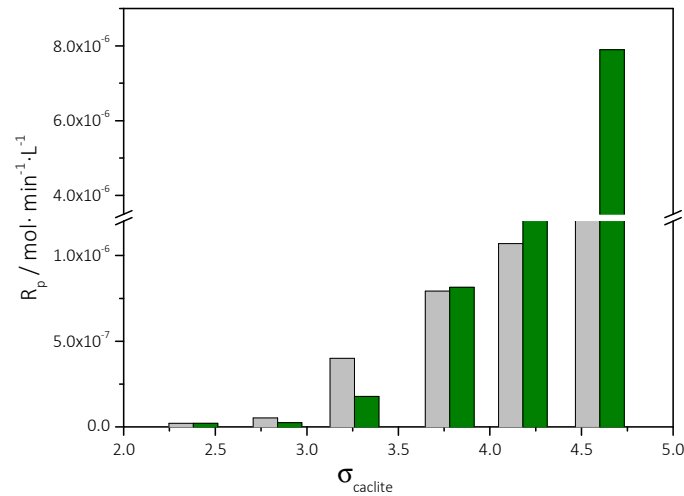


Figure 13. Precipitation of CaCO₃ in supersaturated solutions at constant supersaturation. Rates of precipitation of CaCO₃, as a function of the relative supersaturation with respect to calcite. In the absence (gray bars) and in the presence of AO culture medium and 5 mL of AO culture; supersaturated solutions with AO and culture medium with illumination (green bars); 25 °C, pH 8.5, NaCl 0.15 M.

The dependence of the rate of calcite precipitation, R_p , as a function of corresponding relative supersaturation, σ_{calcite} , is shown in Figure 14. Fitting of the data to the semiempirical power law:

$$R_p = k_p \sigma_{\text{calcite}}^n \tag{5}$$

where k_p and n are the apparent constant and the apparent order of the precipitation, respectively. k_p is a function of the active sites for crystal growth and n is indicative of the mechanism of precipitation. Fitting of the data in Equation (5) suggested that $n = 11$. The meaning of the high value for the apparent order is that the mechanism of CaCO₃ precipitation is described according to the polynuclear model, according to which several nuclei are formed and grow simultaneously on the substrate. The data were fitted to respective rate expression for the polynuclear model [28]:

$$R_p = C_f(SR_{\text{calcite}}) \exp\left(-\frac{\beta \gamma_s^2 V_m^{4/3}}{3(kT)^2 \ln SR_{\text{calcite}}}\right) \tag{6}$$

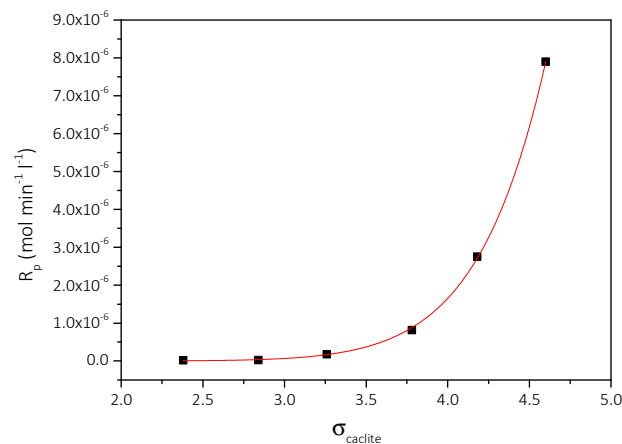


Figure 14. Precipitation of CaCO₃ in supersaturated solutions at constant supersaturation, in the presence of culture medium and 5 mL of AO culture, under illumination. Precipitation rate as a function of relative supersaturation; pH 8.5, 25 °C, NaCl 0.15 M.

In Equation (6) C is a constant, $f(S)$ is a function of the saturation ratio:

$$f(SR_{\text{calcite}}) = SR_{\text{calcite}}^{7/6} (SR_{\text{calcite}} - 1)^{2/3} \ln(SR_{\text{calcite}})^{1/6} \quad (7)$$

β is a shape factor ($b = 1$ in this case), γ_s the surface energy of the nuclei forming at the active growth sites, V_m , the molecular volume of the solid growing, k is Boltzmann's constant and T the absolute temperature.

The plot of $\ln\left(\frac{R_p}{f(SR_{\text{calcite}})}\right)$ as a function of $1/\ln(SR_{\text{calcite}})$ is shown in the plot of Figure 13. The excellent fit suggested that in the presence of AO cultures the growth of calcite is described satisfactorily with the polynuclear model.

From the slope of the linear fit according to Equation (6), shown in Figure 15, the surface energy of calcite was calculated equal to $56 \text{ mJ}\cdot\text{m}^{-2}$.

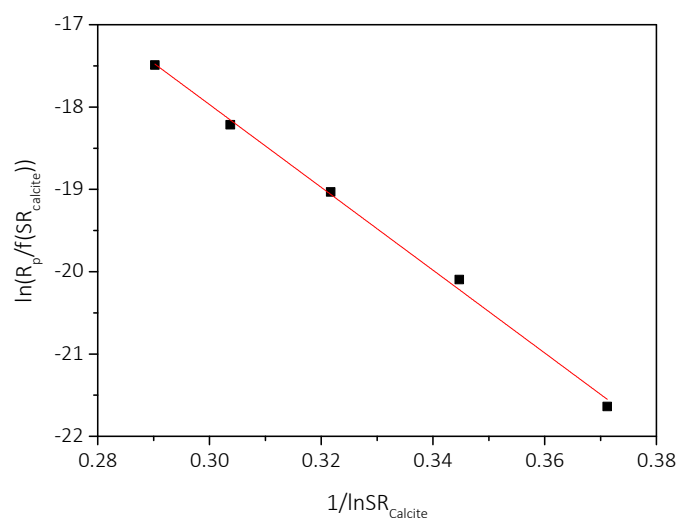


Figure 15. Precipitation of CaCO_3 in supersaturated solutions at constant supersaturation, in the presence of medium and 5 mL of AO culture, under illumination. Plot of the precipitation rates as a function of relative supersaturation, according to the polynuclear model; pH 8.5, 25 °C, NaCl 0.15 M.

3.3. Precipitation of CaCO_3 in Supersaturated Solutions Inoculated with AO Cultures

The selectivity of AO microalgae to induce crystal growth of CaCO_3 was examined in supersaturated solutions, using the free drift method, described in Section 2.2.1. From the results presented so far, it may be suggested that photosynthesis is important for the precipitation of CaCO_3 . Therefore, the role of photosynthesis needs further investigation. The formation of CaCO_3 was induced by the inoculation of the supersaturated solutions with substrates that possess the active sites needed for the nucleation and subsequent growth of an insoluble salt. For example, the inoculation of supersaturated CaCO_3 solutions with calcite seed crystals is known to induce crystal growth of calcite without nucleation [29]. When the inoculation solids are different than calcite, the existence of a nucleation barrier is anticipated. Four different substrates were used to inoculate the supersaturated CaCO_3 solutions: (i) AO microalgae, dried at 70 °C for 24 h ($\text{SSA} < 0.1 \text{ m}^2\cdot\text{g}^{-1}$), (ii) AO microalgae, air dried at 25 °C for 2 days ($\text{SSA} = 2.64 \text{ m}^2\cdot\text{g}^{-1}$), (iii) AO culture grown on calcite crystals dried at 25 °C for 2 days ($\text{SSA} = 0.38 \text{ m}^2\cdot\text{g}^{-1}$) and (iv) calcite crystals precipitated on dry AO microalgae, dried at 25 °C ($\text{SSA} = 2.2 \text{ m}^2\cdot\text{g}^{-1}$).

The study was done in the range of relative supersaturation with respect to calcite, 2.38–4.6 (corresponding to Total calcium, $\text{Ca}_t = \text{Total Carbonate}$, C_t range 3.5–6 mM) for ionic strength 0.15 M NaCl. Following the inoculation of the supersaturated solutions with the study substrates, the pH value was monitored.

Inoculation of the supersaturated solutions with AO culture dried at 70 °C for 24 h, did not induce precipitation of CaCO_3 over the range of supersaturations studied as shown

by the stability of pH of the solutions and the calcium concentration in the supersaturated solutions. The lack of precipitation may be due to the denaturation of proteins and reduction of the active sites, which may be ionized functional groups on the cell membranes [30].

Dried AO culture, which is not able to carry out photosynthesis producing chlorophyll was used to inoculate supersaturated solutions, to test its ability to induce nucleation of CaCO_3 . At temperatures exceeding 40–45 °C, the rate of photosynthesis decreases rapidly [31]. Apparently, the activity of the cells was canceled because of the change in the conformation of protein and lipid molecules present in the cell membranes, which are responsible for inducing nucleation and growth of CaCO_3 . As may be seen from the examination of the morphology with SEM, presented in Figure 16, the inactivation of the microalgae could possibly be due to the lysis of its cells associated with enzymatic hydrolysis. The destruction of the cell membranes as well as the components of the extracellular polymeric membrane, most likely contribute to the precipitation of CaCO_3 . It has been shown that membrane destruction accompanied by structural alterations, may also be caused by the exposure of microalgae to ultrasound or under conditions of intense homogenization [32].

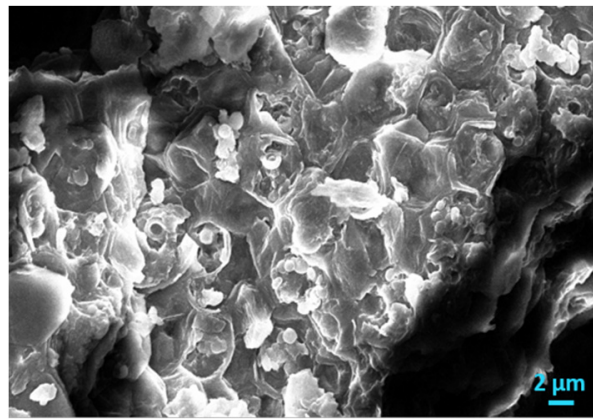


Figure 16. Scanning electron microscope (SEM) photos of AO culture cells, dried at 70 °C.

In the range of supersaturation values with respect to calcite, $2.38 < \sigma_{\text{calcite}} < 4.6$, the solutions, were inoculated with 100 mg of air-dried AO (BET SSA $2.64 \text{ m}^2 \cdot \text{g}^{-1}$) (25 °C). The precipitation was monitored for 24 h.

The profiles of the pH and total calcium, Ca_t are shown in Figure 17a,b.

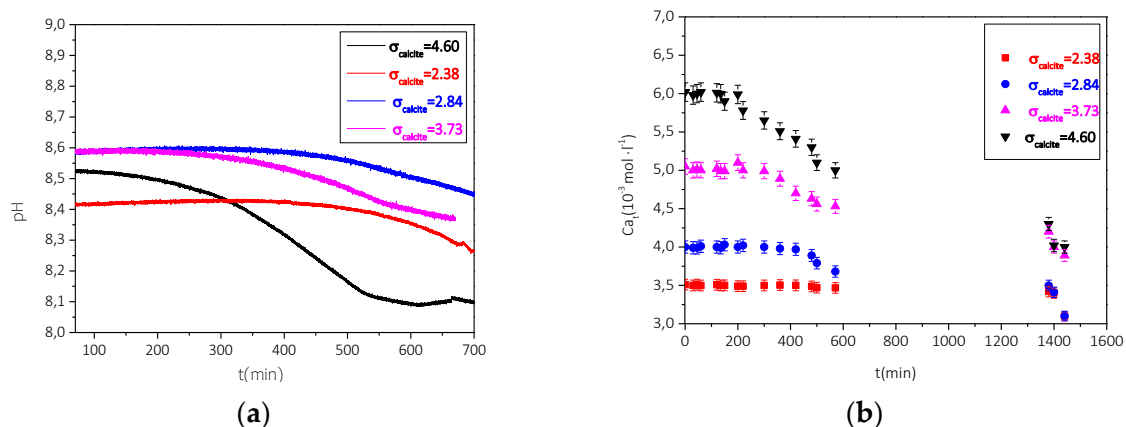


Figure 17. Precipitation of CaCO_3 in supersaturated solutions inoculated with 100 mg air dried AO. (a) Change of pH as a function of time. Initial pH 8.5, 25 °C, 0.15 M NaCl & (b) Calcium (total), Ca_t as a function of time pH 8.5, 25 °C, 0.15 M NaCl.

As may be seen from the pH- time and Ca_t - time profile the precipitation was preceded by induction times inversely proportional to the relative supersaturation of the solutions with respect to calcite. The rates of precipitation were calculated from the Ca_t -time profiles at $t \rightarrow 0$ (initial rates). The conditions at which $CaCO_3$ precipitated following inoculation with air-dried AO cells, the measured induction times, and the rates of precipitation calculated are summarized in Table 4.

Table 4. Precipitation of $CaCO_3$ in stable supersaturated solutions, inoculated with, 100 mg of air-dried AO. Concentration (total) of calcium and total carbonate relative supersaturation with respect to calcite, induction times measured, and rates of $CaCO_3$ precipitation; pH 8.5, 25 °C, 0.15 M NaCl.

Total Calcium, $Ca_t = \text{Total Carbonate}, C_t \times 10^{-3} \text{ mol} \cdot \text{L}^{-1}$	Relative Supersaturation, σ_{calcite}	Induction Time, $t_{\text{ind}}/\text{min}$	Precipitation Rate ($t \rightarrow 0$) / $10^{-6} \text{ mol} \cdot \text{min}^{-1} \cdot \text{L}^{-1} \cdot \text{m}^{-2}$
3.5	2.38	463	1.1
4.0	2.84	406	2.4
5.0	3.73	359	3.1
6.0	4.60	272	5.3

From the XRD patterns obtained, it was found that the solid formed was calcite and vaterite for relative supersaturation values higher than 3.73 (Supplementary Material Figure S1).

It should be noted that the formation of amorphous $CaCO_3$ (ACC) was identified, suggesting that at $\sigma_{\text{calcite}} = 2.38$, this unstable phase was stabilized as verified by XRD and SEM (Supplementary Material Figure S2). The formation of ACC mediated by microorganisms has been reported both in nature [33] and in laboratory studies [34]. It should be noted that ACC was converted into vaterite within the first hour or two and completely to calcite past 24 h of contact of the solid with the mother supersaturated liquor.

Next, the inoculation of the supersaturated solutions with AO culture developed on calcite crystals was investigated. The solid (BET SSA $0.38 \text{ m}^2 \cdot \text{g}^{-1}$) was air-dried past 24 h of culture development and was used to inoculate supersaturated $CaCO_3$ solutions, $2.38 < \sigma_{\text{calcite}} < 4.60$. The precipitation of $CaCO_3$ in the respective supersaturated solutions lasted for 24 h.

In this case, the substrate used to inoculate the supersaturated solutions failed to induce the precipitation of $CaCO_3$.

As already mentioned, (Section 3.2.1), the precipitation of $CaCO_3$ takes place in air-dried AO culture. The mixed calcite-air-dried AO culture solid (BET SSA $2.2 \text{ m}^2 \cdot \text{g}^{-1}$) was used to inoculate supersaturated solutions ($2.38 < \sigma_{\text{calcite}} < 4.60$). The precipitation of $CaCO_3$ was monitored from pH and total calcium concentration as a function of time (free drift). The experimental conditions measured induction times preceding precipitation, and the rates (initial) of $CaCO_3$ precipitation are summarized in Table 5.

Table 5. Precipitation of $CaCO_3$, in stable supersaturated solutions, inoculated with 100 mg of calcite-AO culture powdered solid; Total Calcium concentration $Ca_t (=C_t, \text{ total carbonate concentration})$, relative supersaturation with respect to calcite, induction time and precipitation rate; Initial pH 8.5, 0.15 M NaCl, 25 °C.

Total Calcium, $Ca_t = \text{Total Carbonate}, C_t \times 10^{-3} \text{ mol} \cdot \text{L}^{-1}$	Relative Supersaturation, σ_{calcite}	Induction Time, $t_{\text{ind}}/\text{min}$	Precipitation Rate ($t \rightarrow 0$) / $10^{-6} \text{ mol} \cdot \text{min}^{-1} \cdot \text{L}^{-1} \cdot \text{m}^{-2}$
3.5	2.38	435	1.7
4.0	2.84	385	3.7
5.0	3.73	242	4.8
6.0	4.60	208	8.3

The precipitate consisted of a mixture of vaterite and calcite. The morphology of the precipitate showed CaCO_3 aggregates, (Figure 18a), in which the calcite rhombohedra (Figure 18b,c), were associated with AO cell remnants (Figure 18d).

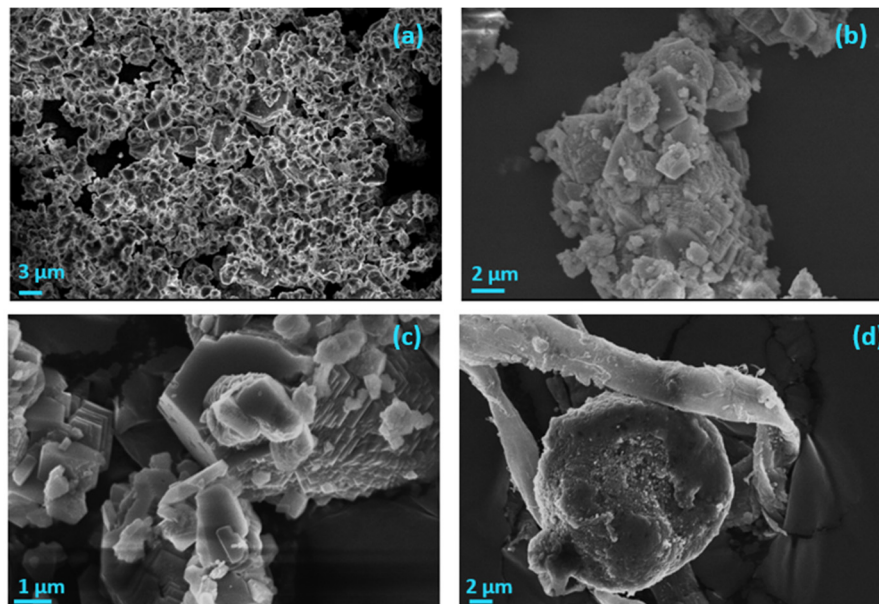


Figure 18. SEM photographs of the precipitate in stable supersaturated solutions of CaCO_3 , $\sigma_{\text{calcite}} = 3.73$, on mixed calcite-air dried AO cells; (a) calcite crystallites aggregate; (b) calcite rhombohedral crystal aggregates; (c) calcite crystals and aggregates; (d) calcite crystallite associated with dry AO cells showing association with cell membrane; pH 8.5, 0.15 M NaCl, 25 °C.

Comparison of the rates of precipitation of CaCO_3 with the corresponding solutions of the same supersaturation were seeded with AO culture dried at 25 °C (air dried) and showed accelerated precipitation upon inoculation with the mixed AO dried culture with CaCO_3 crystals, as may be seen in Figure 19.

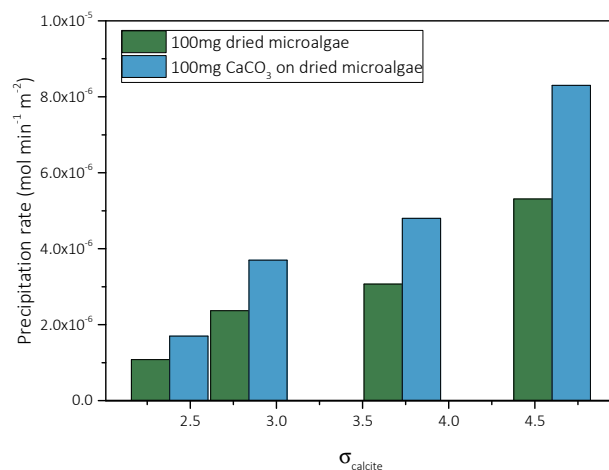


Figure 19. Rate of precipitation of CaCO_3 in stable supersaturated solutions inoculated with air-dried AO culture (green bars) and with mixed calcite precipitated in air dried AO culture (blue bars), as a function of supersaturation; Initial pH 8.5, 0.15 M NaCl, 25 °C.

4. Conclusions

Acutodesmus Obliquus (AO) cultures were grown under periodic illumination (light:dark = 16:8), in the aqueous nutrient medium Basal Bold's Medium, at pH 6.5 and temperature 25 °C. The growth of AO was monitored from measurements of the produced chlorophyll.

The ability of AO cultures to induce selectively the precipitation of calcium carbonate (CaCO_3) from stable CaCO_3 supersaturated solutions was tested by monitoring the free-drift precipitation in supersaturated solutions. For AO obtained in suspension form, the number of cells was very important. The rates of precipitation of CaCO_3 increased linearly with AO culture cells as a function of time. The rates of CaCO_3 precipitation in the presence of AO and the respective nutrients of AO increased by up to 79% when the supersaturated solutions were illuminated, most likely because of the increase in AO cell concentration and contribution from the CO_2 production from the photosynthesis activity. Air dried ($25\text{ }^\circ\text{C}$) AO culture induced the precipitation of CaCO_3 from stable supersaturated solutions because the cells and cell membranes provided the necessary active sites for the nucleation and crystal growth of CaCO_3 . On the contrary, AO culture cells dried at $70\text{ }^\circ\text{C}$, did not show any activity with respect to the selective growth of CaCO_3 , because of the denaturation of the cell membrane components (proteins-lipids). It is interesting to note, that CaCO_3 precipitated because of the presence of air-dried AO cells stabilized amorphous CaCO_3 (ACC) which with time was converted to more stable CaCO_3 , such as vaterite and calcite. The latter was the only CaCO_3 polymorph identified past contact with the mother supersaturated aqueous solution for 24 h.

Supplementary Materials: The following supporting information can be downloaded at: <https://www.mdpi.com/article/10.3390/biomimetics7040140/s1>, Figure S1: Precipitation (free drift) of calcium carbonate in supersaturated solutions ($\text{SR}_{\text{calcite}} = 11.48$), at constant temperature, $25\text{ }^\circ\text{C}$, in the presence of 100 mg of AO culture, dried in ambient air. X-ray diffraction pattern of the precipitated solid; Figure S2: SEM photo of calcium carbonate precipitated in supersaturated solutions ($\text{SR}_{\text{calcite}} = 11.48$), at a constant temperature of $25\text{ }^\circ\text{C}$ with free change of concentrations, in the presence of 100 mg of dry microalgae, dried in ambient air at $25\text{ }^\circ\text{C}$.

Author Contributions: P.D.N., contributed to the acquisition, analysis, and interpretation of data and drafted the work. P.G.K., contributed with the conceptualization, supervision of the work, SEM work and writing of the final submitted. All authors have read and agreed to the published version of the manuscript.

Funding: Partial funding provided by the General Secretariat for Research and Technology (GSRT) and the Hellenic Foundation for Research and Innovation (HFRI) in the context of the action “1st Proclamation of Scholarships from HFRI for PhD Candidates”.

Institutional Review Board Statement: Not applicable.

Data Availability Statement: Not applicable.

Acknowledgments: The authors are grateful for the support by the General Secretariat for Research and Technology (GSRT) and the Hellenic Foundation for Research and Innovation (HFRI) in the context of the action “1st Proclamation of Scholarships from HFRI for Ph.D. Candidates.

Conflicts of Interest: The authors declare no conflict of interest.

References

1. Walker, J.; Surman, S.; Jass, J. *Industrial Biofouling Detection, Prevention and Control*; Wiley: New York, NY, USA, 2000; p. 15.
2. Fingerman, M.; Nagabhushanam, R.; Thompson, M.F. *Recent Advances in Marine Biotechnology*; Enfield, N.H., Ed.; Science Publishers, Inc.: Hauppauge, NY, USA, 1999; p. 168.
3. Donlan, R.M. Biofilms: Microbial Life on Surfaces. *Emerg. Infect. Dis.* **2002**, *8*, 883–890. [[CrossRef](#)]
4. Bixler, G.D.; Bhushan, B. Biofouling: Lessons from nature. *Phil. Trans. R. Soc. A* **2012**, *370*, 2381–2417. [[CrossRef](#)]
5. Amy, G. Fundamental understanding of organic matter fouling of membranes. *Desalination* **2008**, *231*, 44–51. [[CrossRef](#)]
6. Flemming, H.C.; Schaule, G. Biofouling on membranes—A microbiological approach. *Desalination* **1988**, *70*, 95–119. [[CrossRef](#)]
7. Bendinger, B.; Rijnaarts, H.H.M.; Altendorf, L.; Zehnder, A.J.B. Physicochemical cell surface and adhesive properties of coryneform bacteria related to the presence and chain length of mycolic acids. *Appl. Environ. Microbiol.* **1993**, *59*, 3937–3977. [[CrossRef](#)] [[PubMed](#)]
8. Tsuneda, S.; Aikawa, H.; Hayashi, H.; Yuasa, A.; Hirata, A. Extracellular polymeric substances responsible for bacterial adhesion onto solid surface. *FEMS Microbiol. Lett.* **2003**, *223*, 287–292. [[CrossRef](#)]
9. Sheng, G.-P.; Yu, H.-Q.; Li, X.-Y. Extracellular polymeric substances (EPS) of microbial aggregates in biological wastewater treatment systems: A review. *Biotechnol. Adv.* **2010**, *28*, 882–894. [[CrossRef](#)]

10. Zhu, T.; Dittrich, M. Carbonate Precipitation through Microbial Activities in Natural Environment, and Their Potential in Biotechnology: A Review. *Front. Bioeng. Biotechnol.* **2016**, *4*, 4. [[CrossRef](#)]
11. Castro-Alonso, M.J.; Montañez-Hernandez, L.E.; Sanchez-Muñoz, M.A.; Macias Franco, M.R.; Narayanasamy, R.; Balagurusamy, N. Microbially Induced Calcium Carbonate Precipitation (MICP) and Its Potential in Bioconcrete: Microbiological and Molecular Concepts. *Front. Mater. Sci.* **2019**, *6*, 126. [[CrossRef](#)]
12. Perito, B.; Mastromei, G. Molecular Basis of Bacterial Calcium Carbonate Precipitation. In *Molecular Biomineralization: Aquatic Organisms Forming Extraordinary Materials*; Müller, W.E.G., Ed.; Springer: Berlin/Heidelberg, Germany, 2011; pp. 113–139.
13. Cam, N.; Georgelin, T.; Jaber, M.; Lambert, J.F.; Benzerara, K. In vitro synthesis of amorphous Mg-, Ca-, Sr- and Ba-carbonates: What do we learn about intracellular calcification by cyanobacteria? *Geochim. Cosmochim. Acta* **2015**, *161*, 36–49. [[CrossRef](#)]
14. Head, I.M.; Gray, N.D.; Babenzien, H.D.; Oliver-Glöckner, F. Uncultured giant sulfur bacteria of the genus *Achromatium*. *FEMS Microbiol. Ecol.* **2000**, *33*, 171–180. [[CrossRef](#)] [[PubMed](#)]
15. Xu, H.; Peng, X.; Bai, S.; Ta, K.; Yang, S.; Liu, S.; Jang, H.B.; Guo, Z. Precipitation of calcium carbonate mineral induced by viral lysis of cyanobacteria: Evidence from laboratory experiments. *Biogeosciences* **2019**, *16*, 949–960. [[CrossRef](#)]
16. Beveridge, T.; Murray, R. Uptake and retention of metals by cell walls of *Bacillus subtilis*. *J. Bacteriol.* **1976**, *127*, 1502–1518. [[CrossRef](#)]
17. Dupraz, C.; Reid, R.P.; Braissant, O.; Decho, A.W.; Norman, R.S.; Visscher, P.T. Processes of carbonate precipitation in modern microbial mats. *Earth-Sci. Rev.* **2009**, *96*, 141–162. [[CrossRef](#)]
18. Silambarasan, T.S.; Bajwa, K.; Dhandapani, R. Optimization and mass culture of *Acutodesmus obliquus* RDS01 under open phototrophic pond cultivation for enhancing biodiesel production. *Biofuels* **2017**, *8*, 243–252. [[CrossRef](#)]
19. Sarwa, P.; Verma, S.K. Identification and Characterization of Green Microalgae, *Scenedesmus* sp. MCC26 and *Acutodesmus obliquus* MCC33 Isolated from Industrial Polluted Site Using Morphological and Molecular Markers. *Int. J. Appl. Sci. Biotechnol.* **2017**, *5*, 415–422. [[CrossRef](#)]
20. Andersen, R.A. *Algal Culturing Techniques*; Elsevier: Cambridge, MA, USA, 2005; ISBN 0-12-088426-7.
21. Rinanti, A.; Kardena, E.; Astuti, D.I.; Dewi, K. Growth response and chlorophyll content of *Scenedesmus obliquus* cultivated in different artificial media. *Asian J. Environ. Biol.* **2013**, *1*, 1–10.
22. Abramoff, M.D.; Magalhaes, P.J.; Ram, S.J. Image Processing with ImageJ. *Biophotonics Int.* **2004**, *11*, 36–42.
23. Kenne, G.; van der Merwe, D. Classification of Toxic Cyanobacterial Blooms by Fourier-Transform Infrared Technology (FTIR). *Adv. Microbiol.* **2013**, *3*, 37921. [[CrossRef](#)]
24. Chiou, Y.T.; Hsieh, M.L.; Yeh, H.H. Effect of algal extracellular polymer substances on UF membrane fouling. *Desalination* **2010**, *250*, 648–652. [[CrossRef](#)]
25. Melcrová, A.; Pokorna, S.; Pullanchery, S.; Kohagen, M.; Jurkiewicz, P.; Hof, M.; Cwiklik, L. The complex nature of calcium cation interactions with phospholipid bilayers. *Sci. Rep.* **2016**, *6*, 38035. [[CrossRef](#)] [[PubMed](#)]
26. Parkhurst, D.L. *User's Guide to PHREEQC: A Computer Program for Speciation, Reaction-Path, Advective-Transport, and Inverse Geochemical Calculations*; Earth Science Information Center, Open-File Reports Section [Distributor]; US Department of the Interior, US Geological Survey: Lakewood, CA, USA; Denver, CO, USA, 1995.
27. Amjad, Z.; Koutsoukos, P.; Tomson, M.B.; Nancollas, G.H. The Growth of Hydroxyapatite from Solution A New Constant Composition Method. *J. Dent. Res.* **1979**, *58*, 1431–1432. [[CrossRef](#)]
28. Nielsen, A.E. Electrolyte crystal growth mechanisms. *J. Cryst. Growth* **1984**, *67*, 289–310. [[CrossRef](#)]
29. Kazmierczak, T.F.; Tomson, M.B.; Nancollas, G.H. Crystal growth of calcium carbonate. A controlled composition kinetic study. *J. Phys. Chem.* **1982**, *86*, 103–107. [[CrossRef](#)]
30. Mathur, S.; Agrawa, D.; Jajoo, A. Photosynthesis: Response to high temperature stress. *J. Photochem. Photobiol.* **2014**, *137*, 116–126. [[CrossRef](#)]
31. Percy, R.W. Acclimation of Photosynthetic and Respiratory Carbon Dioxide Exchange to Growth Temperature in *Atriplex lentiformis* (Torr.) Wats. *Plant Physiol.* **1977**, *59*, 795–799. [[CrossRef](#)]
32. Wang, D.; Li, Y.; Hu, X.; Su, W.; Zhong, M. Combined Enzymatic and Mechanical Cell Disruption and Lipid Extraction of Green Alga *Neochloris oleoabundans*. *Int. J. Mol. Sci.* **2015**, *16*, 7707–7722. [[CrossRef](#)]
33. Jones, B.; Peng, X. Amorphous calcium carbonate associated with biofilms in hot spring deposits. *Sediment. Geol.* **2012**, *269–270*, 58–68. [[CrossRef](#)]
34. Borowitzka, M.A.; Larkum, A.W.D.; Nockolds, C.E. A scanning electron microscope study of the structure and organization of the calcium carbonate deposits of algae. *Physiologia* **1974**, *13*, 195–203. [[CrossRef](#)]